Experimental Research on Influencing Factors and Ratio Optimization of New High Fluidity Borehole Sealing Material

Xin GUO, Sheng XUE*, Chunshan ZHENG,* Yaobin LI

Abstract: This paper takes the fluidity of the sealing material as the main research indicators. Using the Design-Expert 8.0.5 trial software designed orthogonal experiments and establishing a quadratic model between liquidity and each test factor, which showed the impact of each key factor on the fluidity, the optimal ratio of high-fluidity borehole sealing materials was obtained. The results showed that the key factors had the following order of significance: water-cement reducing agent > water-cement ratio > retarder > expansion agent, comprehensive consideration of expansion rate, compressive strength and setting time. The optimal percentages were found for the high-fluidity borehole sealing material: a water-cement ratio of 1, along with 0.03% retarder, 0.5% water reducer, and 8% expansion agent. These research results could provide a reference for improving the performance of gas drainage borehole sealing materials and enhancing the effect of gas drainage.

Keywords: borehole sealing material; high fluidity; optimal ratio; orthogonal experiment; significance

1 INTRODUCTION

China has a high frequency of gas disaster accidents. With the increasing mining depth of coal resources, China is faced with increasingly serious gas problems, which pose a serious threat to the safety and efficiency of coal mining [1-3]. In order to prevent gas accidents during coal mining, gas pre-drainage technology is usually used to extract the gas from coal seams. However, the effect of gas drainage in China is generally poor. In addition to the low air permeability of the coal seam, the performance of the borehole sealing material also affects the drilling and sealing effect to a large extent. The borehole sealing materials commonly used in China's coal mines include cement mortar and polyurethane materials. However, these materials have poor penetration in micro fissures smaller than 0.1 mm, and the cracks are closed under high stress [4], resulting in poor sealing effects. This requires a borehole sealing material with good fluidity to allow it to be effectively injected into the fine cracks in the coal and rock mass [5-6]. Ultra-fine cement prepared by refining ordinary cement particles can meet the injection requirements for fine cracks. Compared with traditional borehole sealing materials, ultrafine cement materials have higher strength, better durability, and non-toxicity [7-9]. However, to ensure that the borehole sealing material can be efficiently injected into the fine cracks of the coal and rock mass, in addition to having high fluidity, it should also have relatively high stability, a certain degree of micro-swelling, and a suitable setting time [10].

Scholars in China and abroad have conducted numerous studies on ultrafine cement. Hogancamp et al. [11] found that carbon nanofibers could increase the shrinkage and crack resistance of ultra-fine cement mortar while maintaining the hardness. Miaoet al. [12] studied the influence of the content and fineness of limestone powder on the rheological properties of cement paste: the fluidity of cement slurry increases with the increase in the content of limestone powder, and the fineness of limestone powder increases. Zhang et al. [13] added 0.56% aluminum powder and 2% gypsum to Portland cement and mixed them with a water-cement ratio of 0.6 to produce a CF sealing material, and compared the new CF sealing material with ordinary cement. There is difference between permeability and fluidity. The research results show that the new CF sealing slurry has better fluidity and permeability than ordinary cement, indicating that the new CF sealing material has better sealing performance than ordinary cement. Wongkornchaowalit et al. [14] studied the influence of polycarboxylic acid superplasticizer on the fluidity of Portland cement. The research results proved that when the polycarboxylic acid superplasticizer was 1.8% - 2.4%, the fluidity of cement has increased substantially. Chen et al. [15] studied the fluidity of ordinary cement materials with different amounts of ultrafine cement. Guo et al. [16] developed a composite ultrafine cement slurry by adding acrylate copolymer R161 and acrylate S400 to ultrafine cement, which showed good stability and injectability. Wang et al. [17] studied the fluidity of cement slurries with different glass fiber ratios. Adding glass fibers to pure cement slurries will reduce the fluidity of pure cement slurries. And with the increase of the glass fiber content, the fluidity of this cement slurry is also lower.

Previous studies on the modification of ultrafine cement had a goal of improving the performance from one aspect, with no modification method simultaneously taking into account high fluidity, expansibility, and strength. This study used ultra-fine silicate ultra-mud as the base material and added a calcium oxide-calcium sulfate composite as a swelling agent, and polycarboxylic acid as a water-reducing agent and retarder, to develop a new type of borehole sealing material that considered the material's compressive strength, fluidity, and swelling rate (the swelling rate of a test block after 60 days of curing). As the basis for judgment, the best admixture and water-to-material ratio were determined using the single factor experiment method and orthogonal experiment method.

2 MATERIALS AND METHODS
2.1 Experimental Materials

The new type of borehole sealing material was based on ultra-fine Portland cement. The ultra-fine cement used in the experiment was produced by Shandong Kangjing New Material Technology. The appearance was a gray powder. The measured D90 value was 12.6 μm, and the measured D50 value was 5 μm. In addition, all the

technical parameters and indicators met the requirements of "Superfine Portland Cement" (GB/T35161-2017). Its chemical composition is provided in Tab. 1. The expansion agent used in this experiment was a calcium oxide-calcium sulfate composite expansion agent (HCSA) produced by Shijiazhuang City Functional Building Materials Co., Ltd., and it had the appearance of an off-white powder. Its components are listed in Tab. 1. The polycarboxylic acid water-reducing agent (PCE) used in the experiment was

produced by FuyangChengnanBuilding Materials Co., Ltd. It was a white powder that was easily soluble in water, and the water reduction rate was 20 - 35%. The retarder used in this experiment was seaweed powder produced by Jiangsu Changzhou Angu Waterproof Material Co., Ltd. The seaweed powder had the appearance of a white powder and was easily soluble in water. The solution was a colorless and transparent viscous liquid. Water was used to formulate a solution with a mass ratio of 1:130.

Table1 Chemical composition of raw materials

Chemical composition	SiO$_2$	Al$_2$O$_3$	Fe$_2$O$_3$	CaO	MgO	SO$_3$	Loss	Total
HCSA expanding agent	4.96	8.52	0.99	64.18	2.67	16.97	1.19	99.48
Superfine Portland cement	20.57	9.89	3.08	57.65	2	2.7	2.6	98.49

2.2 Experimental Method

Researchers have found that the addition of a retarder [18] can enable to control the setting time, and HCSA [19-21] will help cement hydration products to form a good spatial structure and improve the expansion performance, while the addition of PCE has a dispersing effect on cement particles and can improve the workability of cement and reduce unit water consumption [22-23]. Use Design-Expert 8.0.5 trial software to design the orthogonal experiment (Tab. 2). A total of 29 sets of experiments were carried out with the four factors and three levels, and the fluidity of the test block was taken as the response value [18, 24-27]. After the completion of the orthogonal experiment, the Design-Expert 8.0.5 trial software was used to calculate the variance and range of the experimental data and study the effect of the compound mixing of various additives on the performance of the sealing material. Finally, a response surface regression analysis was performed on the results of the orthogonal experiment and a quantitative regression model reflecting the relationship between the compound dosing amount of the admixture and each filling performance index was obtained, which provided a basis for the optimization of the borehole sealing material formulation [28].

In the experiment, the standard triple test mold (70.7 mm × 70.7 mm × 70.7 mm) was first prepared. Then, the dry material and water quantities required for the production of the test piece were calculated according to the proportions in Tab. 2 and Tab. 3. After mixing with water, the weighed ultra-fine cement, expansion agent, and water-reducing agent were added together and mixed thoroughly. Finally, water was added for thorough mixing and pouring into the mold (Fig. 1), which was placed in the curing box for curing (temperature 20 ± 2°C, humidity above 95%).

Figure 1 Preparation of sample

The fluidity test of the borehole sealing material was conducted using the specified determination method for

cement mortar fluidity (GB/T2419-2005), which was expressed by the diffusion diameter (mm) of the slurry on a horizontal glass plate. The truncated cone mold had an upper mouth diameter of 36 mm, a lower mouth diameter of 60 mm, and a height of 60 mm. The evenly stirred cement slurry was placed in a round mold, the surface was flattened, and the round mold was quickly lifted off. After the cement slurry flowed, the average of the two perpendicular diameters was measured as the maximum fluidity (Fig. 2).

Figure 2 Cement fluidity test

The standard cement consistency water consumption, setting time, and stability test method (GB/T1346-2011) were used to measure the setting time. TUse cement slurry standard consistency setting time tester (Vicat meter) to measure setting time. First zero the Vicat meter. Then, water was separately added to the new borehole sealing material, which was evenly mixed and poured into test molds, and placed in the curing box for curing after being leveled. Finally, the initial and final setting times of the material were measured according to the national standard.

Different materials were added to pure cement and mixed to form cement slurries. After molding, the initial volume was recorded as V1. The volume was read at corresponding time intervals, and the expansion rate was tested for two months.

$$\varepsilon_t = \frac{V_n - V_1}{V_1} \times 100\% \tag{1}$$

The sample strength test utilized the standard cement mortar strength inspection method (GB/T50080-2016), with an RMT uniaxial press used to test the compressive strength of samples with different ages. Place the test piece on the lower plate or back plate of the testing machine and start the testing machine. During the test, the load should be applied continuously and evenly. When the test piece is about to fail and begin to quickly deform, please stop adjusting the throttle of the testing machine until it fails. Then record the load.

Use Design-Expert software to analyze the test results. First click the Analysis button to test the significance of the linear function, 2FI model, second-order model, and third-order model, and pass the model significance test, lack of fit item detection, and correlation. Compare the tested data and recommend a suitable model. Then (click the ANOVA button) to perform analysis of variance and significance test according to the selected model. In the analysis of variance, the significance of the constant term, the first term, the quadratic term (interaction term), and the square

term (surface effect) that affect the quadratic equation model will be tested. By analyzing the response surface curve and contour map, it can be intuitively seen that the model has extreme points and the range of corresponding optimal process parameters. You can also use the software optimization function. Click the Optimization button in the Design-Expert software, and then click Numerical, and select the maximum response value within the range of experimental factors to optimize the best conditions.

Table 2 Value range of each factor in orthogonal experiment

Test group	Value range of each factor/%			
	Water–cement ratio	Retarder	Water-reducing agent	Expanding agent
ZJ1-29	0.8 - 1.0	0.03 - 0.05	0.3 - 0.5	8 - 10

3 RESULTS AND DISCUSSION
3.1 Model Establishment

First, it was necessary to select a suitable model to fit the results, and the results of the orthogonal experiment (listed in Tab. 3) were input into the Design-Expert 8.0.5 software to fit different models. The fitting results are listed in Tab. 4 and Tab. 5. The Design-Expert software recommended the use of linear equation models and quadratic equation models, which had better fits than other models. From Tab. 4, it can be seen that the linear equation

and quadratic equation models had larger F values. The Prob > F values were small, indicating that the two fitting models were the most significant. At the same time, it can be seen from Tab. 5 that the sum of the squared prediction residuals is low in several models. However, the R^2 value of the linear model is 0.685, which is smaller than the R^2 value of the quadratic equation model (0.9144), indicating that the model's correlation with the experimental results is low.

Table 3 Orthogonal test results

NO	A	B / %	C / %	D / %	R_{3d} / MPa	R_{7d} / MPa	R_{28d} / MPa	Fluidity / mm	Initial setting time / min	Final setting time / min	Expansion rate / %
1	0.8	0.03	0.4	9	29.899	32.069	41.597	213.5	440	469	1.897
2	0.8	0.04	0.5	9	37.697	38.477	42.833	226	419	437	2.032
3	0.8	0.04	0.4	10	30.986	32.991	38.969	190.5	410	430	3.281
4	0.8	0.04	0.3	9	33.997	35.01	39.021	199	406	443	1.931
5	0.8	0.04	0.4	8	39.918	42.197	41.398	185.5	431	458	1.593
6	0.8	0.05	0.4	9	31.652	34.133	37.256	207.5	461	490	1.821
7	0.9	0.03	0.5	9	28.479	32.141	36.966	242	343	376	1.898
8	0.9	0.03	0.4	10	26.943	28.511	34.981	218.5	344	368	2.471
9	0.9	0.03	0.4	8	30.931	32.871	38.996	234	416	438	1.614
10	0.9	0.03	0.3	9	27.696	31.233	37.061	179	337	370	1.521
11	0.9	0.04	0.4	9	28.601	30.381	36.983	193	430	456	2.053
12	0.9	0.04	0.4	9	28.601	30.381	36.983	193	430	456	2.053
13	0.9	0.04	0.3	10	31.239	32.011	34.882	153.5	424	449	2.329
14	0.9	0.04	0.4	9	28.601	30.381	36.983	193	430	456	2.053
15	0.9	0.04	0.5	8	34.312	38.021	37.409	212	437	463	1.589
16	0.9	0.04	0.5	10	31.213	32.997	34.411	243	422	444	2.809
17	0.9	0.04	0.3	8	32.986	36.021	37.311	183.5	431	457	1.621
18	0.9	0.04	0.4	9	28.601	30.381	36.983	193	430	456	2.053
19	0.9	0.04	0.4	9	28.601	30.381	36.983	193	430	456	2.053
20	0.9	0.05	0.3	9	25.896	28.033	33.767	153.5	482	518	1.621
21	0.9	0.05	0.5	9	26.062	29.133	36.761	247	360	395	1.812
22	0.9	0.05	0.4	10	26.993	27.012	33.761	167	365	393	2.597
23	0.9	0.05	0.4	8	28.922	30.41	34.562	185	490	525	1.531
24	1	0.04	0.3	9	27.664	29.008	33.678	179	420	454	1.986
25	1	0.03	0.4	9	26.295	28.091	32.019	240	349	376	1.778
26	1	0.04	0.4	10	26.513	27.978	28.072	230	359	386	2.093
27	1	0.05	0.4	9	23.997	27.843	31.907	229.5	475	503	1.803
28	1	0.04	0.4	8	28.911	31.036	38.213	207.5	439	463	1.302
29	1	0.04	0.5	9	27.476	29.989	33.778	280	422	457	1.889

Table 4 ANOVA results of different models

Source	Sum of Squares	df	Mean Square	F Value	p - value Prob > F	
Mean vs Total	1.229E + 006	1	1.229E+006			
Linear	16806.13	4	4201.53	13.04	< 0.0001	Suggested
2FI	2615.00	6	435.83	1.53	0.2236	
Quadratic	3015.67	4	753.92	5.03	0.0101	Suggested
Cubic	1884.63	8	235.58	6.58	0.0169	
Residual	214.77	6	35.80			
Total	1.254E + 006	29	43239.47			

Table 5 Comprehensive statistical analysis of multiple models

Source	Std. Dev.	R - Squared	Adjusted R - Squared	Predicted R - Squared	PRESS	
Linear	17.95	0.6850	0.6324	0.5231	11701.95	Suggested
2FI	16.86	0.7915	0.6757	0.3841	15111.63	
Quadratic	12.25	0.9144	0.8289	0.5072	12092.52	Suggested
Cubic	5.98	0.9912	0.9592	−0.2605	30927.00	

Thus, the model is inaccurate. The *Adj R²* value of the linear model is small compared with that of the quadratic equation model, indicating that the model still needs further development. Based on these results, the experiment initially selected the quadratic equation model for fitting.

3.2 Model Verification

Although the conformity degree of each model was compared when the model was selected, the comparison terms (*F* value, R^2, etc.) were relatively abstract. Therefore, it was still necessary to verify the selected model in other ways. The studentized residual was used to draw a comparison between the predicted residual value and the actual value (Fig. 3). The abscissas of the points on the map were mostly concentrated in the center, and the distribution of the points was also approximately a straight line, indicating that the model prediction was reliable.
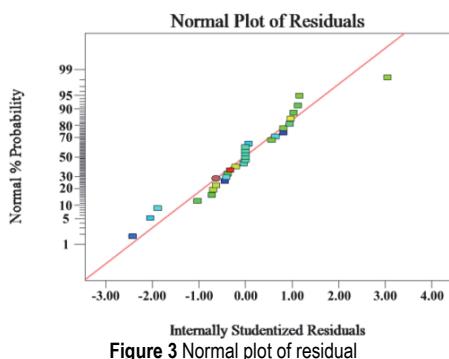
Figure 3 Normal plot of residual

3.3 Variance Results and Significance Tests

From Tab. 6, it can be seen that the F value of the model is 10.69, the Prob > *F* value is less than 0.0001, and the correction coefficient of determination (Adj *R*2) is 0.8289, which shows that the model fits the data well and the experimental error is small. From the significance test, it can be seen that the factors had the following order of significance: *C* (water-reducing agent) > *A* (water-cement ratio) > *B* (retarder) > *D* (expansion agent). The factor combinations had the following order: *AC* (water-cement ratio, water-reducing agent) > *CD* (water-reducing agent, expansion agent) > *BC* (retarder, water-reducing agent) > *AD* (water-cement ratio, expansion agent) > *AB* (water-cement ratio, expansion agent) > *BD* (retarder, expansion agent). Among these, the Prob > *F* value of the *C* factor was less than 0.0001, which indicated that the index was extremely significant, and the Prob > *F* values of factors *A* and *B* were less than 0.005, which indicated that these two indicators were significant; the interaction of *AC* was the most significant, and the interaction of *BD* was the least significant.

Table 6 Response surface quadratic model and analysis of variance results

Source	Sum of Squares	df	Mean Square	F	Prob > F	Significance
Model	22436.79	14	1602.63	10.69	< 0.0001	***
A	1728.00	1	1728.00	11.52	0.0044	**
B	1575.52	1	1575.52	10.51	0.0059	**
C	13500.52	1	12838.02	90.03	< 0.0001	***
D	2.08	1	2.08	0.014	0.9078	*
AB	5.06	1	5.06	0.034	0.8569	*
AC	1369.00	1	1369.00	9.13	0.0092	**
AD	76.56	1	76.56	0.51	0.4866	*
BC	232.56	1	232.56	1.55	0.2334	*
BD	1.56	1	1.56	0.010	0.9201	*
CD	930.25	1	930.25	6.20	0.0259	**
A²	2200.05	1	2200.05	14.67	0.0018	**
B²	582.84	1	582.84	3.89	0.0688	*
C²	327.37	1	327.37	2.18	0.1617	*
D²	95.32	1	95.32	0.64	0.4386	*
Residual	2099.40	14	149.96			
Lack of Fit	2099.40	10	209.94			
Pure Error	0.000	4	0.000			
Cor Total	24536.19	28				
			The values of Prob in this article represent the significant degree of influence of all factors on liquidity.*** *P* value (−∞, 0.0001) ; **P* value (0.0001, 0.05) ; *P* value (0.05, +∞)			

3.4 Response Surface Analysis

The response surface drawn according to the binomial polynomial regression equation was a three-dimensional surface obtained by the interaction of the response values of the independent variables. The response value (liquidity) could be predicted and optimized, and any two factors could also be adjusted to analyze their interaction and

obtain the interaction rules. It was possible to determine when any two of the four factors (A (water-cement ratio), B (retarder content), C (water-reducing agent content), and D (expansion agent content)) remained unchanged by the interaction and laws of the other two factors.

Fig. 4 shows the effect of the water-cement ratio and water-reducing agent on the fluidity results. It can be seen from Fig. 4 that the fluidity varies greatly with the water-cement ratio or water-reducing agent, and the response surface is steep at this time. As reflected in the contour map, the contour lines are dense. The rapid color change in the contour map also proves that the slope of the response surface is large. This indicates that the water-cement ratio and interaction of the water-reducing agent have a significant impact on the response value, which is consistent with the previous variance analysis results for each item. The two factors of the ash ratio and water-reducing agent have a more significant influence on the test results.

Fig. 5 shows the effect of the water-reducing agent and expansion agent on the fluidity results. It can be seen from Fig. 5 that when the water-reducing agent and expansion agent are taken at the upper limits of their selected level ranges, the fluidity change trend is relatively steep, indicating that the interaction between the time-reducing agent and expansion agent has a significant impact on the response value. The contour distribution trend is related to the factor level, and there is a certain distortion in the three-dimensional surface graph. The interaction of these two factors affects the particle flow, and the dense contour lines on the abscissa also indicate that the water-reducing agent has a greater impact on fluidity.

Fig. 6 shows the effect of the retarder and water-reducing agent on the fluidity results. It can be seen from Fig. 6 that the contour lines on the ordinate are denser, while the contour lines on the abscissa are sparse, indicating that the retarder has a greater impact on fluidity. When the upper limit of the content of the retarder is used, the response surface is relatively smooth, indicating that the retarder has a certain influence on the fluidity, but the range of this influence is small.


Figure 4 Effect of water-cement ratio and water reducer on fluidity
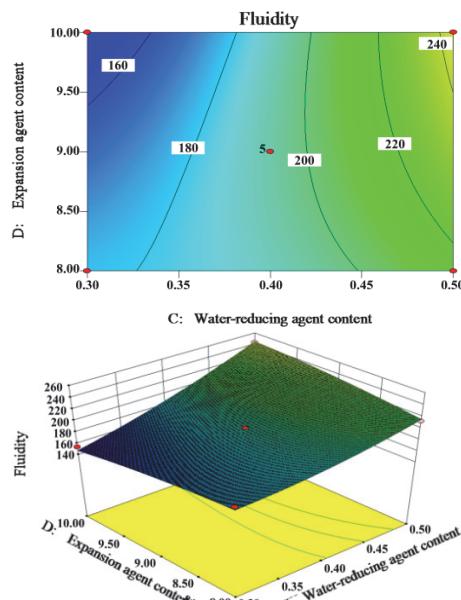
Figure 5 Effect of water-reducing agent and expansion agent on fluidity
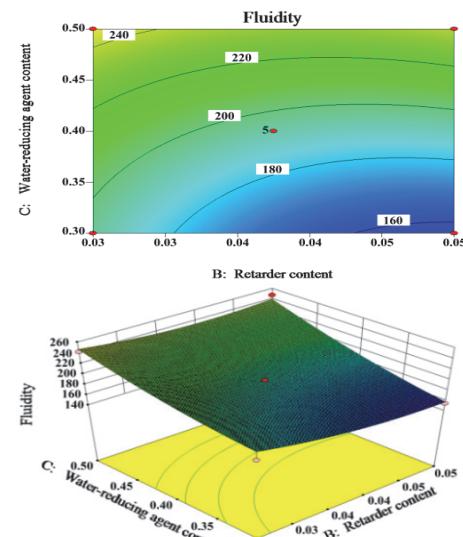
Figure 6 Effect of retarder and water-reducing agent on fluidity
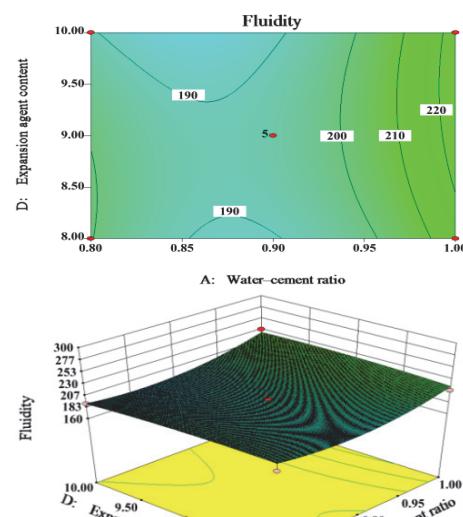

Figure 7 Effect of water-cement ratio and expansion agent on fluidity

Fig. 7 shows the effect of the water-cement ratio and expansion agent on the fluidity results. It can be seen from Fig. 7 that the contour lines of the ordinate are sparse and the contour lines of the abscissa are dense, indicating that the water-cement ratio has a greater impact on the fluidity. The expansion agent has little effect on the fluidity; the

response surface is relatively smoother, indicating that the interaction of the two factors has a certain impact on the fluidity, but the range of this influence is small. When using the upper limits of the two factors, the response surface is steep, indicating that the interaction of the two factors has the greatest impact on the liquidity at this time.
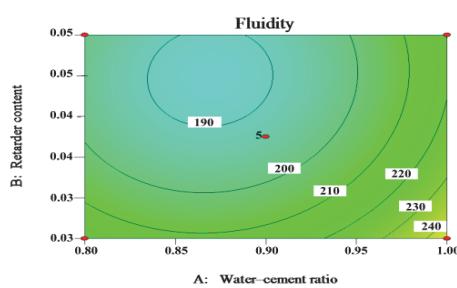
**Figure 8** Effect of water-cement ratio and retarder on fluidity
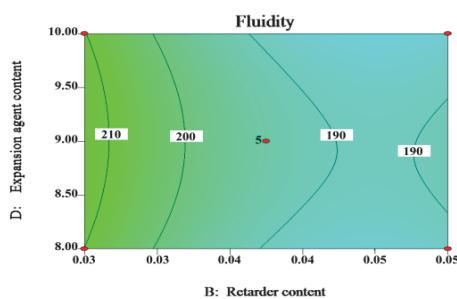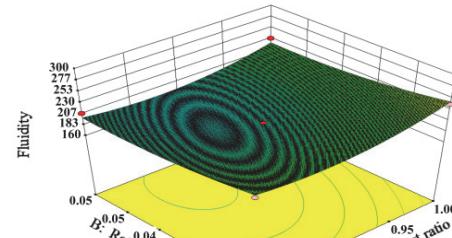
**Figure 9** Effect of retarder and expansion agent on fluidity
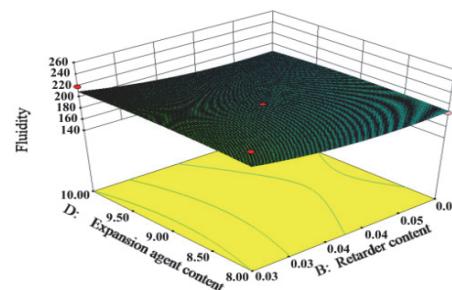
Fig. 8 shows the effect of the water-cement ratio and retarder on the fluidity results. The shape of the contour reflects the strength of the interaction effect. A circle indicates that the interaction of the two factors is not significant, while an ellipse shows the opposite. It can be seen from Fig. 8 that the distribution of the abscissa contour lines is denser than that on the ordinate, indicating that the influence of the water-cement ratio on the response value is more significant than that of the retarder. The pattern change law is similar to the response obtained by the two-factor analysis of variance in the figure. The influence law of the value is the same, and the graph has a certain distortion. When the water-cement ratio is at the upper limit and the retarder is at the lower limit, the response surface is steep, but the overall response surface is relatively flat, indicating a certain interaction between the two factors, but the effect is small.

Fig. 9 shows the effect of the retarder and expansion agent on the fluidity results. As shown in Fig. 9, the contour

lines on the abscissa are dense, while the contour lines on the ordinate are sparse, indicating that the influence of the coagulant on the fluidity is greater than that of the expansion agent. This is consistent with the results of the analysis of variance, and the response surface is the smoothest when the retarder interacts with the expansion agent, indicating that the interaction between the retarder and expansion agent has the least significant effect on the fluidity.

3.5 Parameter Optimization and Verification

The Design-Expert software was used for further analysis of the experimental results, using the fluidity as the optimization index to obtain the optimized experimental program by selecting the first six groups of optimized experimental programs, and verifying them, as shown in Tab. 7.

Table 7 Optimization scheme and results

NO	Experimental optimization ratio				Forecast liquidity / mm	Measured liquidity / mm	Error / %
	Water-cement ratio	Retarder / %	Water reducing agent / %	Expansion agent / %			
1	1	0.03	0.5	8.00	288.494	288.4	−0.034
2	0.99	0.03	0.49	9.11	287.832	287	−0.289
3	0.98	0.04	0.5	9.98	287.561	287.5	−0.021
4	1	0.03	0.49	9.06	288.624	286.5	−0.736
5	0.97	0.03	0.49	9.98	283.282	283.5	0.077
6	0.98	0.03	0.49	9.82	287.186	287	−0.065

4 CONCLUSION

(1) Using ultrafine cement as the base material, adding expansion agent, polycarboxylic acid water reducer and

retarder, developed a sealing material that meets the requirements of fluidity and expansion performance. It can be seen from the results of the response surface that as the water-cement ratio increases, the fluidity of the material

also increases. As the content of retarder increases, the fluidity of the drilling seal material continues to decrease. As the amount of water reducing agent increases, the fluidity of the material increases. As the amount of expansion agent increases, the fluidity of the test block decreases.

(2) Orthogonal experiments were designed using the Box-Behnken module in the Design Expert software. Fluidity was the response value, and various test factors (water-cement ratio, water-reducing agent, retarder, and expansion agent) were established and optimized. The quadratic model of time showed a high prediction accuracy.

(3) The influence of each component on the fluidity of the material was obtained using a range and variance analysis and a significance test. These had the following order: *C* (water-reducing agent) > *A* (water cement ratio) > *B* (retarder) > *D* (expansion agent).

(4) According to the response surface drawn by the binomial polynomial regression equation, the interaction of any two factors was analyzed, and the interaction laws were obtained. These effects had the following order: *AC* (water-cement ratio, water-reducing agent) > *CD* (water-reducing agent, expansion agent) > *BC* (retarder, water-reducing agent) > *AD* (water–cement ratio, expansion agent) > *AB* (water-cement ratio, retarder) > *BD* (retarder, expansion agent).

(5) Combining the orthogonal test results of the response surface analysis method with the fluidity test results of the sealing material, the best experimental conditions for the test are obtained: the water-reducing agent content is 0.5%, the retarder content is 0.03%, and the water-cement ratio is 1, and the expansion agent content is 8%.

Acknowledgements

5   REFERENCES

[1] Yuan, L. (2016). Strategic thinking of simultaneous exploitation of coal and gas in deep mining. *Journal of China Coal Society*, *41*(1), 1-6.

[2] Yuan, L. & Zhang, P. S. (2019). Development status and prospect of geological guarantee technology for precise coal mining. *Journal of China Coal Society*, *44*(8), 2277-2284.

[3] Kang, H. P. (2014). Support technologies for deep and complex roadways in underground coal mines: A review. *International Journal of Coal Science & Technology, 1*(3), 261-277. https://doi.org/10.1007/s40789-014-0043-0

[4] Wtrzykowshi, M., Trtik, P., Munch, B., Weiss, J., Vontobel, P., & Lura, P. (2015). Plastic shrink age of mortars with shrink age reducing admixture and lightweight aggregates studied by neutron tomography. *Cement and Concrete Research*, *73*, 238-245. https://doi.org/10.1016/j.cemconres.2015.03.013

[5] Pantazopoulos, I. A., Markou, I. N., Christodoulou, D. N., Droudakis, A. I., Atmatzidis, D. K., Antiohos, S. K., & Chaniotakis, E. (2012). Development of microfine cement grouts by pulverizing ordinary cements. *Cement and Concrete Composites*, *34*(5), 593-603. https://doi.org/10.1016/j.cemconcomp.2012.01.009

[6] Gahle, C. & Kutter, H. K. (2003). Breakage and shear behaviour of intermittent rock joints. *International Journal of Rock Mechanics and Mining Sciences*, *40*(5), 687-700. https://doi.org/10.1016/S1365-1609(03)00060-1

[7] Wu, A. X., Yu, S. F., Han, B., Wang, Y. M., Huang, M. Q., & Wang, Y. (2014) Optimization of mix-proportion and diffusing rule of super-fine cement grouting slurry. *Journal of Mining & Safety Engineering*, *31*(2), 304-309.

[8] Zhang, J. P., Liu, L. M., Zhang, F. T., & Cao, J. Z. (2018). Development and application of new composite grouting material for sealing groundwater inflow and reinforcing wall rock in deep mine. *Scientific Reports*, *8*(1), 1-8. https://doi.org/10.1038/s41598-018-23995-y

[9] Wang, K., Wang, L. G., Lu, Y. L., Sun, X. K., & Zhang, K. W. (2020). Visual experimental study on the infiltration effect of cement slurry in micro-fractures. *Journal of China Coal Society*, *45*(3), 990-997.

[10] Guo, D. M., He, T. Y., Yang, R. S., Ye, D. S., Zhang, Y. Q., & Li, C. P. (2017). CT analysis on micro-cement grouting effect for fractured rock sample. *Journal of Mining & Safety Engineering*, *34*(5), 987-992.

[11] Hogancamp, J. & Grasley, Z. (2017). The use of microfine cement to enhance the efficacy of carbon nanofibers with respect to drying shrinkage crack resistance of portland cement mortars. *Cement & Concrete Composites*, 83, 269-272. https://doi.org/10.1016/j.cemconcomp.2017.08.006

[12] Miao, M., Xue, K. W., Miao, F., & Jiang, W. H. (2018). Influence of Limestone Powder on Hydration Characteristics and Rheological Properties of Cement Paste. *Journal of Hunan University (Natural Sciences)*, *45*(12), 90-96.

[13] Zhang, C., Chang, J., Li, S. G., Liu, C., Qin, L., Bao, R. Y., Liu, H., & Cheng, R. H. (2019). Experimental study comparing the microscopic properties of a new borehole sealing material with ordinary cement grout. *Environmental Earth Sciences*, *78*(5), 149. https://doi.org/10.1007/s12665-019-8165-8

[14] Wongkornchaowalit, N. & Lertchirakarn, V. (2011). Setting Time and Flowability of Accelerated Portland Cement Mixed with Polycarboxylate Superplasticizer. *Journal of Endodontics, 37*(3), 387-389. https://doi.org/10.1016/j.joen.2010.11.039

[15] Chen, J. J. & Kwan, A. K. H. (2012). Superfine cement for improving packing density, rheology and strength of cement paste. *Cement & Concrete Composites*, *34*(1), 1-10. https://doi.org/10.1016/j.cemconcomp.2011.09.006

[16] Guo, Y. C., Shen, A. Q., Ma, L., Zhu, J. H., & Wang, X. F. (2010). Microstructure of crack filling material of polymer emulsion superfine cement. *Journal of Chang'an University(Natural Science Edition)*, *30*(1), 16-22.

[17] Wang, Q. B., Zhu, Q. K., Shao, T. S., Yu, X. G., Xu, S. Y., Zhang, J. J., & Kong, Q. L. (2018). The rheological test and application research of glass fiber cement slurry based on plugging mechanism of dynamic water grouting. *Construction and Building Materials*, *189*, 119-130. https://doi.org/10.1016/j.conbuildmat.2018.08.081

[18] Du, H. C., Wang, Y. N., He, M. M., Lin, Z. F., & Lyu, Z. Z. (2019). Study on the Effect of Organic Retarder on the Performance of Cement Modified Emulsified Asphalt Mastic. *Materials Review*, *33*(S2), 254-260.

[19] Huang, Z. Y., Liu, Y. Q., & Li, C. W.(2015). Performance Research of Ultra High Performance Concrete Incorporating HCSA Expansion Agent. *Materials Review*, *29*(4), 116-121.

[20] Li, B., Xu, L. H., Gu, Y. S., & Jia, M. L. (2017). Investigation on influence of HCSA expansive agent on dosage on performance of high-strength self-compacting concrete. *Engineering Journal of Wuhan University*, *50*(1), 90-96.

[21] Feng, J. J., Miao, M., & Yan, P. Y. (2012). Hydration and Expansion Properties of Shrinkage-Compensating Composite cementitious Materials. *Journal of Building Materials*, *15*(4), 439-445.

[22] Shui, L. L., Yang, H. J., Sun, Z. P., He, Y., & Zeng, W. B. (2019). Study on Effect Rate and Influencing Factors of Dispersion Effect of Different Types of Superplasticizer. *Journal of Building Materials*, *22*(6), 853-859.

[23] Du, R. R., Zhang, X., Gu, M. D., & Ji, T. (2019). The Composition Effect and Mechanism of Polycarboxylate Superplasticizers and Early Strength Agent. *Materials Review*, *33*(7), 2461-2466.

[24] Yu, X., Yu, C., Ran, Q. P., & Liu, J. P. (2018). Retarding Mechanism of Hydroxy Carboxylic Acid Retarder on Cement Hydration. *Journal of the Chinese Ceramic Society*, *46*(2), 181-186.

[25] He, T. S. & Li, Z. K. (2015). Study on Influences of Polycarboxylate Superplasticizer on Performance of low cement Castable. *Materials Review*, *29*(S1), 351-353, 365.

[26] Shui, L. L., Sun,Z. P., Yang, H. J., Yang, X., Ji, Y. L. & Luo, Q. (2016). Experimental evidence for a possible dispersion mechanism of polycarboxylate-type superplasticisers. *Advances in Cement Research*, *28*(5), 287-297. https://doi.org/10.1680/jadcr.15.00070

[27] You, B. & Li, N. Z. (2005). *Expansive agent and shrinkage-compensating concrete*. Beijing, China Building Materials Industry Book.

[28] Lan, W. T., Wu, A. X., & Wang, Y. M. (2019). Formulation optimization and formation mechanism of condensate expansion and filling composites. *Acta Materiae Compositae Sinica*, *36*(6), 1536-1545.

Contact information:

Xin GUO, Postgraduate
School of Safety Science and Engineering,
Anhui University of Science and Technology,
No. 168 Taifeng Street, 232001 Huainan, Anhui Province, China
E-mail: guoxin190510@163.com

Sheng XUE, Prof
(Corresponding author)
School of Safety Science and Engineering,
Anhui University of Science and Technology,
No.168 Taifeng Street, 232001 Huainan, Anhui Province, China
E-mail: sheng.xue@aust.edu.cn

Chunshan ZHENG, PhD
(Corresponding author)
School of Safety Science and Engineering,
Anhui University of Science and Technology,
No.168 Taifeng Street, 232001 Huainan, Anhui Province, China
E-mail: chunshanzheng@aust.edu.cn

Yaobin LI, PhD
School of Safety Science and Engineering,
Anhui University of Science and Technology,
No.168 Taifeng Street, 232001 Huainan, Anhui Province, China
E-mail: binyaoli@163.com